Mass-resolved ion energy measurements at both electrodes of a 13.56 MHz plasma in CF4

Mass-resolved ion energy measurements at both electrodes of a 13.56 MHz plasma in CF_4

R. J. M. M. Snijkers, M. J. M. van Sambeek, M. B. Hoppenbrouwers, G. M. W. Kroesen, and F. J. de Hoog
Eindhoven University of Technology, Department of Applied Physics, P.O. Box 513, 5600 MB Eindhoven, The Netherlands

(Received 13 December 1995; accepted for publication 5 March 1996)

The ion energy distributions (IEDs) at the electrodes in a capacitively coupled 13.56 MHz plasma in CF_4 have been measured mass resolved with a Balzers quadrupole in combination with a home-built energy analyzer. Mass-resolved determination offers the possibility to compare the IED of different ions achieved in the same sheath. The IEDs have been determined at both the largest and the smallest electrode. Apart from the IEDs of the CF_4 species, the IEDs of ionic species in plasmas in argon and nitrogen also were determined. Apart from the CF_4 ionic species CF_3^+, CF_2^+, CF^+, and F^+, CHF_2^+ ions also are present in the CF_4 plasma due to residual water in the reactor. Because the CHF_2^+ ions are not produced in the sheath and because we do not detect elastically scattered ions, the IEDs of these ions show the typical bimodal distribution for rf plasmas which corresponds to an IED of ions which have not collided in the sheath. From these IEDs we can obtain the sheath characteristics, such as the averaged sheath potential. From the IEDs of CF_n^+ ions one can conclude that, in the sheath of the CF_4 plasma, a large number of chemical reactions takes place between the CF_n^+ ions and the neutrals. © *1996 American Institute of Physics.* [S0021-8979(96)00712-8]

I. INTRODUCTION

Radio-frequency (rf) plasmas are commonly used in industry for surface modification processes, e.g., for etching and deposition of semiconductor surfaces in the manufacturing of integrated circuits. These processes are caused by species which are produced in the low-pressure rf plasma glow and which are transported across the sheath, toward the substrate on the electrode surface. The bombardment of the surface by energetic ions is essential to achieve anisotropic etching results.[1,2] The etching process usually takes place at the smallest powered electrode.

An important parameter in the process is the ion energy distribution (IED) at the electrode. The IED depends on parameters such as the ion density profile in the sheath, the mean kinetic electron energy, the cross sections for collisions taking place in the sheath, and thickness and voltage of the sheath. If in a low-pressure rf plasma the sheath may be regarded as collisionless the IED is saddle structured due to the time modulation of the sheath voltage drop. This has been shown experimentally[3–8] as well as theoretically.[6,8–11] The splitting of the saddle structure decreases with increasing excitation frequency of the plasma.

In the collisional case, where the mean free path of the ions is of the same order of magnitude as the sheath thickness, collisions in the sheath have a large influence on the IED. Charge exchange collisions between ions and neutrals cause extra peak structures in the IED at energies lower than the energy of the collisionless saddle structure. This also has been demonstrated both experimentally and theoretically.[6,8,12–14] Elastic scattering of ions by neutrals does not cause any extra peak structures in the IED but results in a broadening.[6–8,14]

In this article measurements of mass-resolved IEDs in a 13.56 MHz plasma in CF_4 are presented. The studied ion species are CF_3^+, CF_2^+, CF^+, F^+, and CHF_2^+. The unexpected presence of CHF_2^+ is attributed to a very small amount of residual water vapor in the reactor. The advantage of the presence of the CHF_2^+ ions is that these ions hardly scatter inelastically. The influence of elastic scattering is known, so the IEDs of CHF_2^+ give information on the sheath structure. From the IEDs of CF_3^+, CF_2^+, CF^+, and F^+, we may conclude in a first-order approach which ion–molecule reactions are important in the sheath.

II. EXPERIMENT

The experimental setup has been described elsewhere.[7,8] The rf plasma is confined in a cylindrical cavity with an electrode area ratio of 3. The driven electrode is ac coupled to the power supply (see Fig. 1). The cavity has been used to measure the electron and negative ion densities by microwave techniques,[15,16] and is created by extending the largest electrode around the plasma towards the smallest. Köhler *et al.*[4] showed that the highest sheath voltage drop appears in front of the smallest electrode, irrespective whether this is the grounded or the driven one.

Because of practical reasons it is difficult to determine the IED at the driven electrode. The mass and energy selector would have to be electrically coupled to the time-dependent electrode potential. There would be severe interference between the rf fields of the plasma and the quadrupole. Therefore, we have measured the IEDs at the grounded electrode and have built two cavities with identical electrode geometries. One has a large and the other a small grounded electrode (see Fig. 2). For historical reasons the situation with the largest electrode grounded is called normal cavity. The other with the smallest electrode grounded is called inverse cavity. Since the potential difference over the electrodes is the same for both configurations when powered

 0021-8979/96/79(12)/8982/11/$10.00

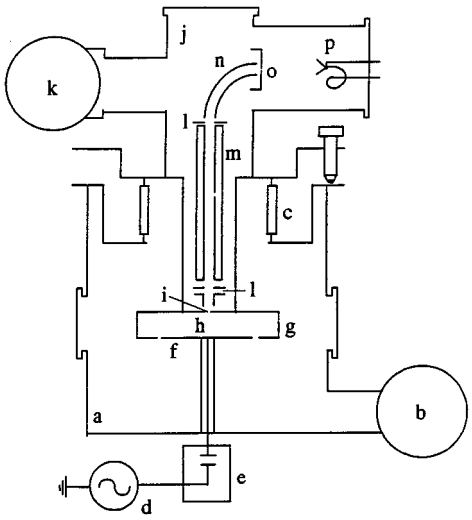

FIG. 1. Schematical view of the diagnostic and the normal cavity. (a) reactor vessel; (b) pump; (c) bellows; (d) rf generator; (e) matching network; (f) rf electrode; (g) grounded electrode; (h) plasma cavity; (i) sample hole; (j) detection chamber; (k) pump; (l) ion lens; (m) quadrupole mass selector; (n) energy selector; (o) exit slit; (p) channeltron.

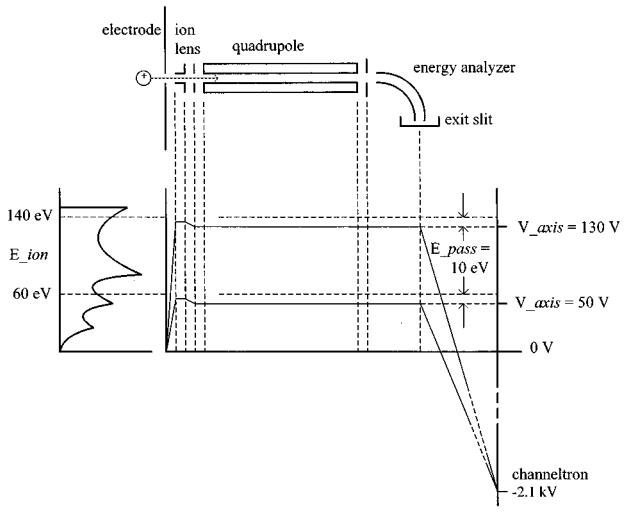

FIG. 3. Schematical view of the reference voltage (V_{axis}) during the measurement of ions with initial an energy of 60 and 140 eV. E_{pass} is fixed at 10 eV. The channeltron voltage is -2.1 kV.

by the same excitation voltage V_{rf}, the plasma is identical in the normal and the inverse cavity.

In an open configuration the plasma potential is constant due to the very large electrode surface ratio. Since in our geometry the surface ratio is only 3, the plasma potential is rf modulated. This effect is larger for the inverse cavity.

A quadrupole mass spectrometer (Balzers QMG311) in combination with a cylindrical mirror energy analyzer is implemented in the grounded electrode. It is situated in a differentially pumped chamber (see Fig. 1). The pressure in this chamber is kept lower than 10^{-6} Torr. In the center of the grounded electrode a small molybdenum plate (diameter 2.5 cm) is mounted with an orifice of 40 μm. Molybdenum is used so no charging of the plate occurs. The pressure in the quadrupole chamber is sufficiently low in order to generate that no modification of the IED take place when ions pass the orifice.[12] Behind the orifice the ions are focused by an ion lens into a beam parallel to the quadrupole axis. The voltages, geometry, and the position of the ion optics have been designed using the computer program SIMION.[17] After mass selection, the ions are energy selected in the cylindrical mirror analyzer. The analyzer has an exit slit of 1 mm, which results in an energy resolution of 1 eV. The resolution of the quadrupole is 0.1 u. The selected ions are detected by a channeltron. After amplification the pulses are counted by a counter card in an IBM-compatible PC.

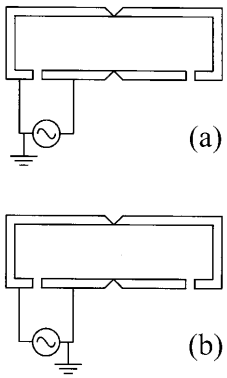

FIG. 2. Schematical presentation of the (a) normal and (b) inverse cavity. The inner diameter of the cavity is 17.5 cm. The diameter of the smallest electrode is 12.5 cm. The inner height of the cavity is 2.0 cm.

Both the resolution and the transmission of the quadrupole and energy selector depend on the kinetic energy of the ions. In order to obtain a constant resolution and transmission during a measurement, ions are accelerated or decelerated by the ion lens before entering the quadrupole, so all ions which are detected have the same kinetic energy when passing the mass and energy selectors. Therefore, the reference (=axis) potential of the total system, including the ion lens, is changed during an energy scan (see Fig. 3), whereas the local electric fields in the quadrupole and energy selector remain the same. The kinetic energy of the ions when passing the analyzing system E_{pass} can be chosen between 5 and 30 eV.

As a consequence of the geometry and the voltage of the ion lens it is only possible to detect ions which hit the electrode surface with a velocity directed nearly perpendicularly to the surface (within an angle of 4° with the normal). It is known that for low-pressure plasmas in which the ion mean free path is larger than the sheath thickness, the sheath is nearly collisionless. Because the ions are accelerated perpendicularly to the electrode, the angular distribution is narrow.[18,19] In this case all the ions that pass the orifice will be within the acceptance angle of 4° and the measured IED corresponds to the real IED.

For the high-pressure case, where the mean free path of the ions is less than the sheath thickness, collisions in the sheath become important. This is the case for pressures higher than 5–10 mTorr. Due to the collisions the angular distribution becomes broader. Ions that do not pass the orifice within the 4° acceptance angle will not be detected and the measured IED may not correspond to the real IED. This

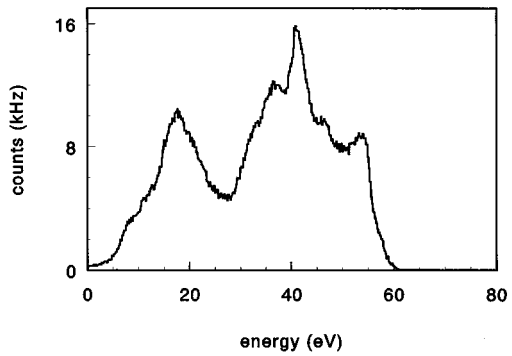

FIG. 4. The IED of Ar^+ ions incident on the grounded electrode in the normal cavity. The pressure is 40 mTorr and the power injected in the plasma is 40 W. The peaks of the primary saddle structure are at 42 and 54 eV.

effect has to be taken into account for the interpretation of the IEDs.

III. THE EFFECT OF COLLISIONS

Charge exchange collisions between a fast ion and a thermal neutral generates a thermal ion and a fast neutral. The newly created ions start with thermal energy (≈ 0) and are accelerated perpendicularly toward the electrode. Due to this effect the ions, which reach the electrode, always hit the electrode surface perpendicularly. Consequently, all these ions pass the ion lens and are analyzed by the spectrometer. Due to the fact that the newly created ions have zero starting energy, these ions generate IED features at lower energies than the primary saddle structure. In an argon plasma, symmetric (resonant) charge exchange takes place between an Ar^+ ion and an Ar neutral,

$$Ar^+ + Ar \rightarrow Ar + Ar^+. \tag{1}$$

The IED of Ar^+ ions measured at the largest electrode in a 40 mTorr plasma in argon is shown in Fig. 4. The peaks of the primary saddle structure are at 42 and at 54 eV. The other features are induced by charge exchange. Symmetric charge exchange for atomic ions has a large cross section[20] on the order of $10-40\times10^{-16}$ cm^2.

The cross section of asymmetric charge exchange between two nonidentical species,

$$A^+ + B \rightarrow A + B^+ \tag{2}$$

is of the order 10^{-17} cm^2.

Also elastic collisions occur frequently in the sheath. The cross section of these collisions is in the order of $5-40\times10^{-16}$ cm^2.[21] In this case the energy of the ion is distributed among the colliding particles. The energy and the direction of the ion will change. Consequently, the ion angular distribution becomes broader[18,21] and most of the ions that are scattered do not hit the electrode within the 4° acceptance angle of the spectrometer.

There is always some residual water vapor in the reactor which is responsible for the formation of hydrogen-containing ions such as ArH^+.[22,23] Due to the fact they have no unpaired electron, the ArH^+ ions are quite stable. Because of the low density of the H_2O molecules, the hydrogen-containing ions hardly have any influence on the space charge in the plasma and the sheath. ArH^+ ions can collide in the sheath with an argon atom and then dissociate or scatter elastically. In the first case, the ArH^+ ion is destroyed and cannot be detected anymore. In the latter case, the direction of the ions is changed and the angular distribution at which the scattered ions hit the electrode is broadened.

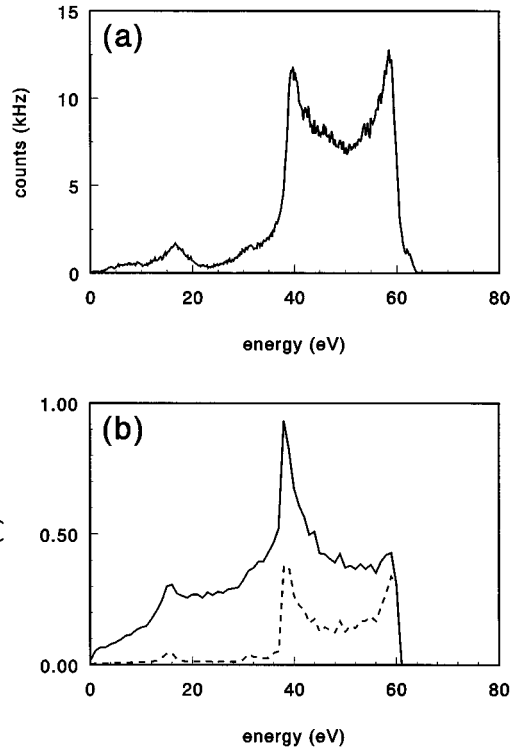

FIG. 5. (a) Measurement and (b) simulation of the IED of ArH^+ ions incident on the grounded electrode in an argon plasma in the normal cavity. The pressure is 40 mTorr and the rf power injected in the plasma is 50 W. The solid line in (b) represents the full angular distribution, whereas the dashed line represents only the detectable $2°\times4°$ cone.

Once again, for the interpretation of the measured IEDs one has to take into account that only those ions are detected which strike the electrode within the 4° acceptance angle of the spectrometer. In the case of elastic scattering, we distinguish three groups of ArH^+ ions that fulfil this condition. The first one consists of ions which do not collide in the sheath. The electric field in the sheath is perpendicular to the electrode, so the ions are accelerated perpendicularly to the electrode. These ions are responsible for the primary saddle structure. The second group consists of ions which lose nearly all their energy during their last collision before they hit the electrode. They behave identically to ions formed by charge exchange collisions and also cause low-energy features in the IEDs. In the case of ArH^+ ions scattered elastically by argon atoms, only head-on collisions satisfy this condition due to the small mass difference between the two species. The energy of the ions in this case is less than the energy related to the saddle structure. The third group consists of ions that, after two or more collisions, are directed perpendicularly to the electrode by coincidence. The energy of the ions in this case is randomly distributed and no peaks are present. The probability that ions end up in the last two

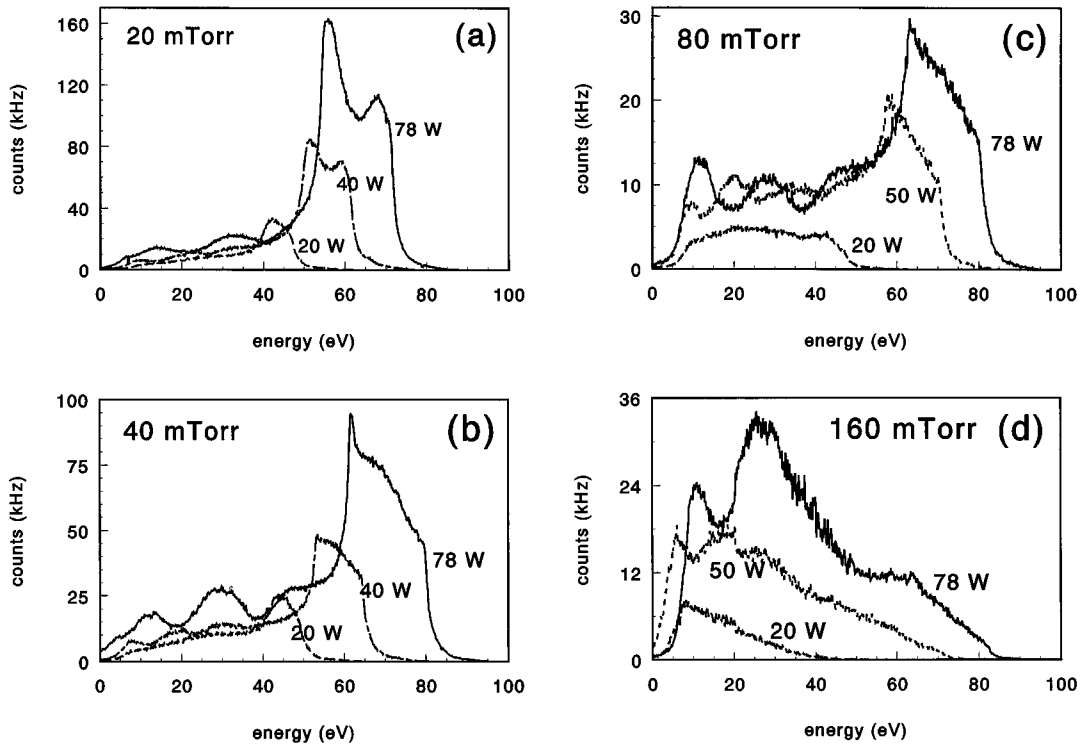

FIG. 6. The IED of CF_3^+ ions incident on the grounded electrode in the normal cavity for several pressure and rf power conditions: (a) 20 mTorr; (b) 40 mTorr; (c) 80 mTorr; and (d) 60 mTorr.

groups is small and we may conclude that the measured IEDs of ArH^+ ions mainly consist of ions which have not collided in the sheath. The measured ArH^+ IEDs show a well-pronounced saddle and may therefore be interpreted as being collisionless and therefore serve as a very illustrative ''probe'' of the determination of the energy range of the primary saddle structure.[7,8]

The effect of the collisions in the sheath has also been demonstrated by simulations. The local and time-dependent electric field in the sheath used in the simulations to calculate the ion trajectories and the ion energy is calculated from solutions of particle-in-cell (PIC) simulations[24,25] and is proved to be close to selfconsistency.[8] Trajectories of 150 000 ions entering the sheath at 200 different phases were calculated. The thickness of the space-charge region is varying in time. The maximum sheath thickness is 1.56 mm and the mean free path is 0.8 mm. The collisions are randomly chosen and are treated as hard sphere elastic scattering where the collision angle in the mass centered system is randomly distributed and the total energy and momentum are conserved.

The measured IED of ArH^+ ions at the largest electrode in a 40 mTorr plasma in argon is shown in Fig. 5(a). The rf power is 50 W. The IED clearly shows the saddle structure whereas small features are noticed at lower energy. These are generated by the elastically scattered ions which bombard the electrode perpendicularly and have lost (nearly) all energy during their last collision. Figure 5(b) shows a simulation of the IED of ArH^+ ions for the same conditions as above. The solid curve represents the full angular distribution of the IED (for experimental data see Thompson *et al.*[26]), while the dotted curve represents the IED of the ions which bombard the electrode within an angle of 4°. The agreement with the measurement is obvious.

IV. RESULTS AND DISCUSSION

A. Introduction

Janes[27] and others already pointed out that the ion dynamics in the sheath of a CF_4 plasma is far more complex than in the case of Ar or N_2. The number of ion species is larger, as is the number of different ion–molecule reactions. This is also a consequence of the abundance of radical species.

In a CF_4 plasma the following positive ions are present: CF_3^+, CF_2^+, CF^+, F^+, C^+, and at higher pressures also $C_2F_5^+$ ions are detected. The presence of CHF_3 molecules in the plasma has been shown by Haverlag[16] using IR techniques. As a result, CHF_2^+ ions are created in the plasma.

Negative ions are also present. These ions, mainly F^-, are trapped in the glow. The density and the temperature of these ions determine the Bohm velocity of the positive ions entering the sheath, but they have no further influence on the dynamics of the positive ions in the sheath. The Bohm velocity in electronegative gases is smaller than in a plasma without negative ions.[8] The consequence of this is that the positive ion density decreases more rapidly toward the electrode than in a plasma without negative ions. Subsequently the sheath thickness is larger than in a plasma without negative ions.

Experimentally determined IEDs of CF_3^+, CF_2^+, CF^+, F^+, and CHF_2^+ ions are presented both for the normal and the inverse cavity case. These results show large differences be-

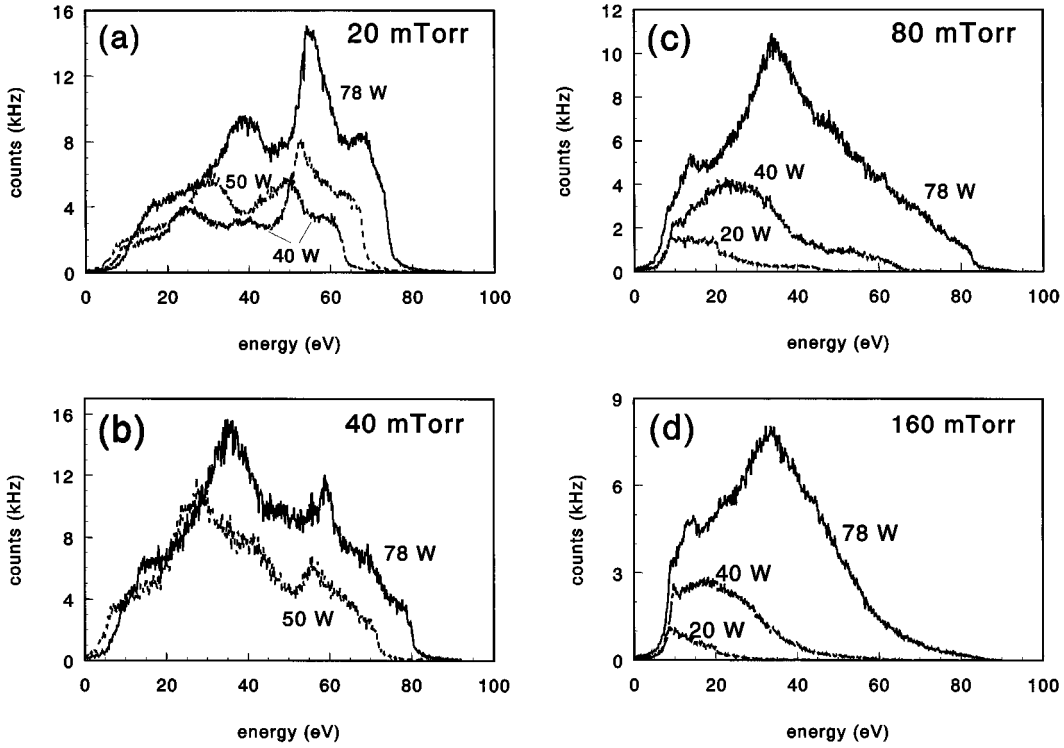

FIG. 7. The IED of CF_2^+ ions incident on the grounded electrode in the normal cavity for several pressure and rf power conditions: (a) 20 mTorr; (b) 40 mTorr; (c) 80 mTorr; and (d) 160 mTorr.

tween the IEDs of the different species. From these results conclusions about the sheath behavior and the ion kinetics in the sheath are derived. It is shown that ions are produced in the sheath. Because of the low electron density in the sheath, these new ions must be formed by ion–molecule reactions.

B. IEDs at the largest electrode

In Figs. 6, 7, 8, 9, and 10, the measured IEDs of CF_3^+, CF_2^+, CF^+, F^+, and CHF_2^+ ions are presented for several plasma conditions in the normal cavity case. The power indicated in the figures means the power injected in the plasma. During these measurements E_{pass} was 20 eV.

The behavior of CHF_2^+ ions is quite similar to ArH^+ ions in an argon plasma: The most probable reactions of CHF_2^+ ions are elastic scattering or an ion–molecule reaction with a CF_4 neutral. In the latter case the ion will be destroyed and cannot contribute to the IED any longer. Once again we remark that the measured spectrum only includes the ions which have hit the electrode surface within an angle of 4°. Because of the mass difference between the CHF_2^+ ion and the CF_4 neutral, the ion will never lose all of its energy when it collides elastically. This means that the measured IED will mainly represent ions which did not collide in the sheath. No elastic scattering features as are occurring in the case of ArH^+ are to be expected.[7,8]

At high pressures the saddle structure is still well recognizable, although the structure is less pronounced than at low pressures (see Fig. 10). At high pressures most of the CHF_2^+ ions are scattered and are not detected. The IEDs of CHF_2^+ ions determined in 5 W plasmas for several pressures do not show a saddle structure but one single peak. This is caused by the fact that at such low power densities the plasma potential is roughly equal to the floating potential. Consequently, the modulation depth of the voltage across the sheath is small: 30%–50%. At higher powers the modulation depth can be as large as 90%–100%; then the saddle structure appears again.

The density of the CF_3^+ ions is expected to be the highest of all the observed ions. When we analyze the IED of the CF_3^+ ions (Fig. 6), we can recognize the primary saddle structure in the low-pressure case (20 and 40 mTorr), whereas this structure vanishes at higher pressures (160 mTorr). In the low-pressure case the IEDs show some small features at energies lower than the saddle structure. These features cannot be generated by elastic scattering because the elastically scattered CF_3^+ ions do not contribute to the measured IED; therefore, the features must be generated by CF_3^+ ions which are created in the sheath. Furthermore, for the newly created ions to arrive at the electrode within the acceptance angle of 4° it is required that they have a starting energy close to 0 eV.

When we consider the IED of CF_2^+ ions in Fig. 7, we can only recognize the primary saddle structure at 20 mTorr. At higher pressures this structure vanishes. This means that the CF_2^+ ions which start from the glow are either scattered elastically or destroyed by chemical reactions. Apparently, in contrast to CF_3^+ ions, the probability for CF_2^+ ions to cross the sheath without any collision is very small. The cross section for elastic scattering of CF_3^+ ions and CF_2^+ ions with CF_4 neutrals will be of the same order. This cannot explain

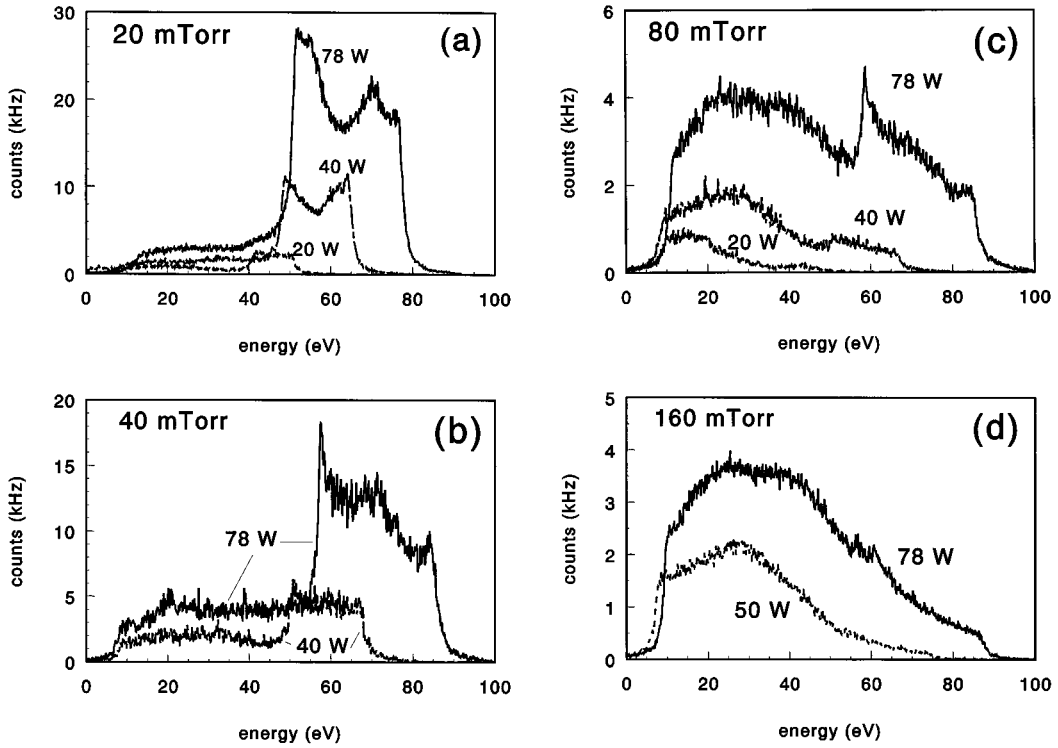

FIG. 8. The IED of CF^+ ions incident on the grounded electrode in the normal cavity for several pressure and rf power conditions: (a) 20 mTorr; (b) 40 mTorr; (c) 80 mTorr; and (d) 160 mTorr.

the different behavior. This means that the CF_2^+ ions have a relatively large chance to be destroyed in the sheath by ion–molecule reactions. This is in agreement with the fact that they have one unpaired electron, while ions such as CF_3^+, CF^+, and CHF_2^+ only have paired electrons. Therefore, the CF_2^+ ions are more reactive. The feature in the IEDs of the CF_2^+ ions at energies smaller than the primary saddle must be generated by production of CF_2^+ ions in the sheath. The pro-

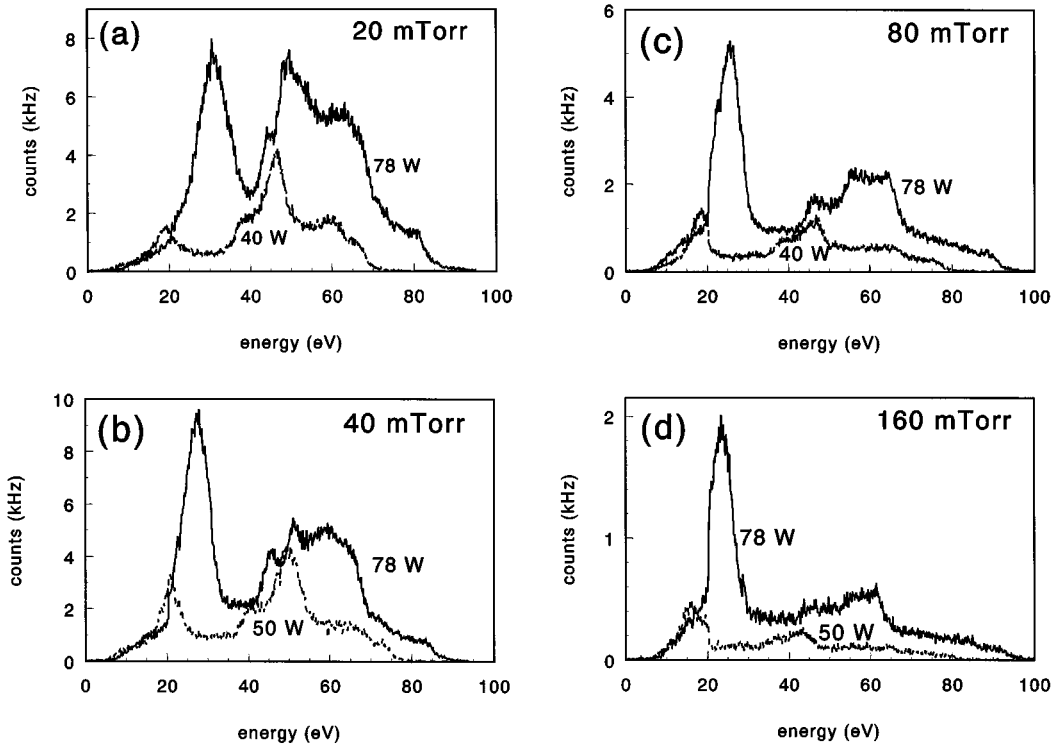

FIG. 9. The IED of F^+ ions incident on the grounded electrode in the normal cavity for several pressure and rf power conditions: (a) 20 mTorr; (b) 40 mTorr; (c) 80 mTorr; and (d) 160 mTorr.

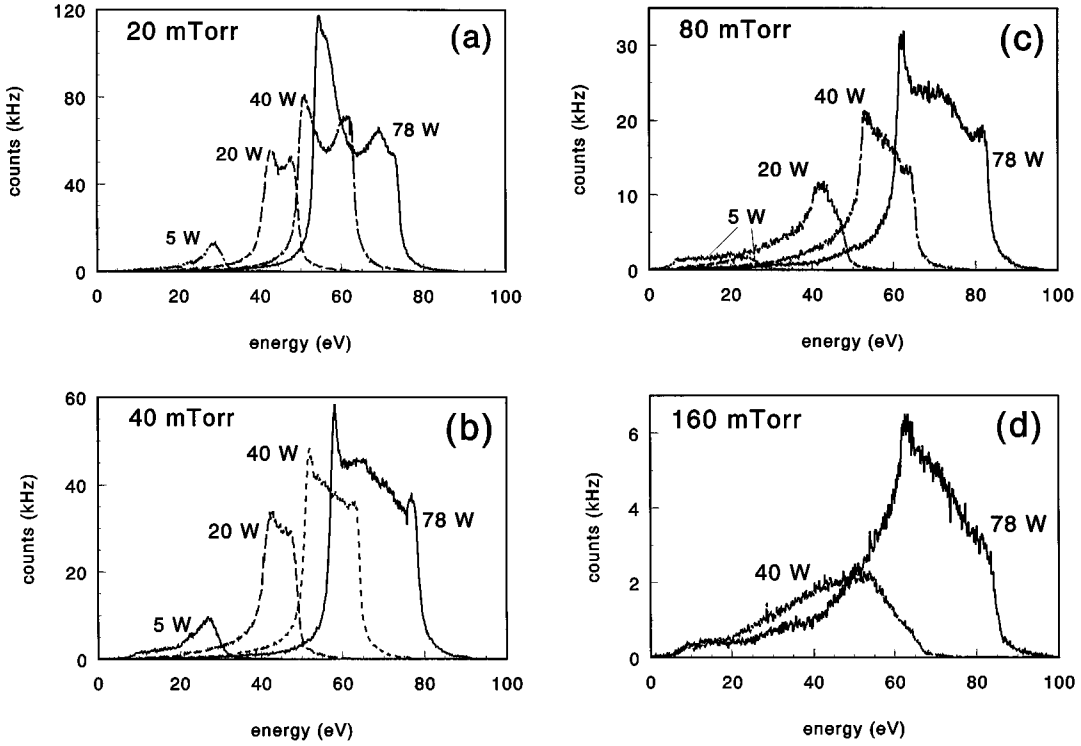

FIG. 10. The IED of CHF_2^+ ions incident on the grounded electrode in the normal cavity for several pressure and rf power conditions: (a) 20 mTorr; (b) 40 mTorr; (c) 80 mTorr; and (d) 160 mTorr.

duction rate is relatively large in order to compensate the rather high loss rate, which is responsible for the vanishing of the primary saddle.

The IEDs of CF^+ ions (see Fig. 8) are similar to those of CF_3^+: The primary saddle structure can be recognized up to about 80 mTorr. The strong increase of low-energy ions at higher pressures can again only be explained by production of forwardly directed ions in the sheath. The smaller number of features is due to the smaller mass of the CF^+ ions with respect to the mass of the CF_3^+ ions, which results in a shorter sheath transit time. The fact that, except for the primary saddle, there are no peak structures may also be the consequence of a possible excess energy after the formation of CF^+ ions.

The primary saddle structure in the IEDs of F^+ ions (see Fig. 9) is recognizable at low pressures (20 and 40 mTorr), while also one very sharp peak can be distinguished up to 160 mTorr. This peak may be produced by ions created in the sheath by ion–molecule reactions or resonant charge exchange reactions. From investigations of Haverlag it is known that the density of *F* neutrals is about five times as high as the CF_3 neutral density.[16] One should take into account that the F^+ ions cannot disappear by dissociation reactions as CF_n^+ ions can.

Several ion–molecule reactions can appear in the CF_4 sheath. From the measured IEDs we may conclude what reactions are dominant. This is discussed in Sec. IV E.

C. IEDs at the smallest electrode

In Figs. 11–13, the IEDs of CF_3^+, CF_2^+, and CF^+ ions are presented as measured in the inverse cavity case in a CF_4 plasma of 5, 14.5, and 72 mTorr, respectively. During these measurements E_{pass} was 33 eV. This is higher than the E_{pass} used in the normal cavity in order to increase the transmission of the spectrometer.

The saddle structure in the IED of CF_3^+ ions is only recognizable at low pressures, up to about 15 mTorr. At higher pressures the saddle vanishes due to the small probability of the ions to cross the sheath without any collision.

The IEDs of CF_2^+ ions do not show any specific features and they look similar for the whole pressure range. The saddle structure has already vanished at pressures as low as 5 mTorr, which corresponds to the results obtained in the normal cavity: The loss rate of CF_2^+ in the sheath is high compared to other ion species. The average energy of the whole

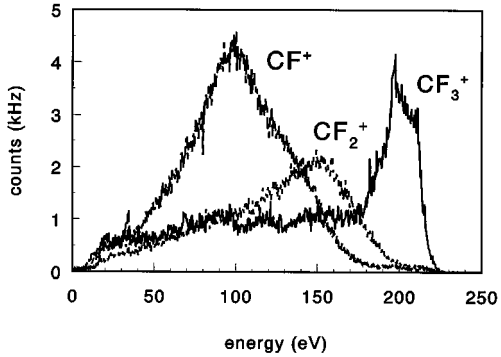

FIG. 11. The IED of CF_3^+ (solid line), CF_2^+ (dashed line), and CF^+ ions (dotted line) incident on the grounded electrode in the inverse cavity. The pressure is 5 mTorr and the rf power injected in the plasma is 85 W.

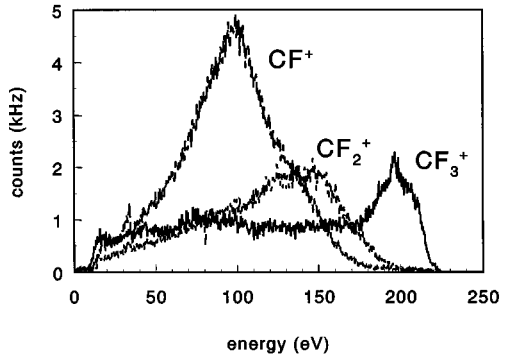

FIG. 12. The IED of CF_3^+ (solid line), CF_2^+ (dashed line), and CF^+ ions (dotted line) incident on the grounded electrode in the inverse cavity. The pressure is 14.5 mTorr and the rf power injected in the plasma is 85 W.

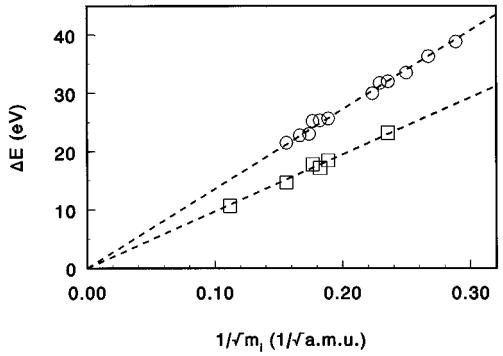

FIG. 14. The relation between the splitting ΔE and the mass of the ion as determined for several ions in a plasma in air. The measurements has been done in the normal (○) and the inverse cavity (□). In both cases the rf power injected in the plasma is 48 W. The pressure in normal cavity case is 80 mTorr, while the pressure in the inverse cavity case is 5 mTorr.

IED decreases with increasing pressure, which is due to the increasing number of collisions in the sheath.

The IEDs of CF^+ ions also look similar for the whole pressure range. The maximum always occurs at about 100 eV. Just like in the CF_2^+ case, the saddle structure has already vanished at 5 mTorr. Hardly any ion can reach the electrode without a collision, and the loss rate in the sheath is higher than the production rate.

In conclusion, the IEDs measured in the inverse cavity show the same features as those measured in the normal cavity; however, the effects induced by collisions in the sheath are enhanced because of the larger sheath thickness.

D. Remarks

When we compare the IED of the normal and of the inverse cavity, we can distinguish a difference in the intensity of the measured distributions. This is partly due to different adjustments of the spectrometer. The main reason, however, of the intensity difference is the number of collisions in the sheath. In the inverse cavity the sheath is thicker due to a higher sheath voltage. Consequently the number of collisions in the sheath increases and the number of ions which do not collide in the sheath (and hit the electrode within the acceptance angle of 4°) decreases.

From the IEDs in which the primary saddle structure can be recognized, the splitting energy difference ΔE can be derived. The splitting energy difference appears to be inversely proportional to $\sqrt{m_i}$ as shown in Fig. 14 for a plasma in air in the normal and inverse cavity. This empirical relation is also valid in pure CF_4, Ar, and N_2 plasmas.[8]

In Fig. 15 the splitting energy difference ΔE of the saddle structure of the IED of CHF_2^+ ions is given as function of the averaged energy of the primary saddle structure E_{sad}. ΔE increases more than linearly with E_{sad}. Based on theoretical investigations,[8] from the increasing ratio between ΔE and E_{sad} we may conclude that the transit time of the ions decreases with increasing E_{sad} and, subsequently, that the sheath becomes thinner with increasing E_{sad}. To generate a thinner sheath at higher sheath voltages, the ion density at the sheath–presheath edge has to increase with increasing E_{sad}.[8]

When we consider ΔE in CF_4 plasmas for different pressure conditions at a certain E_{sad}, we see that ΔE is the largest at the lowest pressures. From this we may conclude that the sheath thickness is the smallest at the lowest pressures: The splitting is larger when the transit time is smaller. The smaller sheath thickness at lower pressures is a consequence of a higher density of the positive ions. Investigations of Haverlag confirm the decrease of the density of the positive ions with increasing pressure.[16] This behavior is in contrast with an argon plasma, where ΔE increases with the pressure

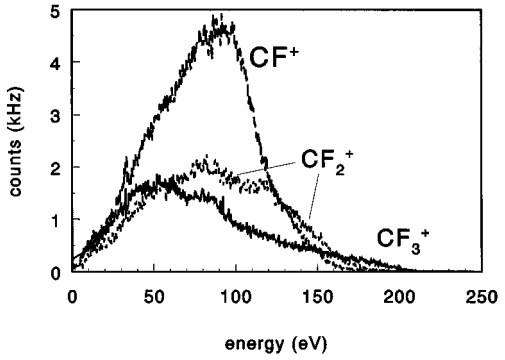

FIG. 13. The IED of CF_3^+ (solid line), CF_2^+ (dashed line), and CF^+ ions (dotted line) incident on the grounded electrode in the inverse cavity. The pressure is 72 mTorr and the rf power injected in the plasma is 85 W.

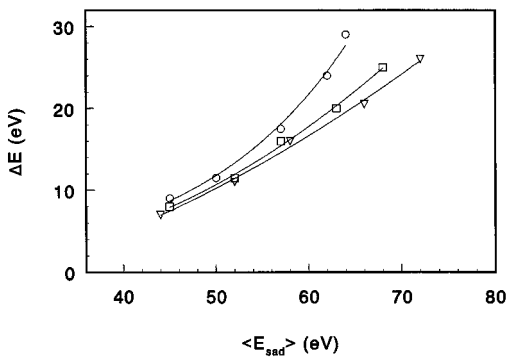

FIG. 15. The relation between $\overline{E_{\mathrm{sad}}}$ and ΔE in the CF_4 plasmas in the normal cavity, determined from the IEDs of the CHF_2^+ ions for 20 (○), 40 (□), and 80 mTorr (▽).

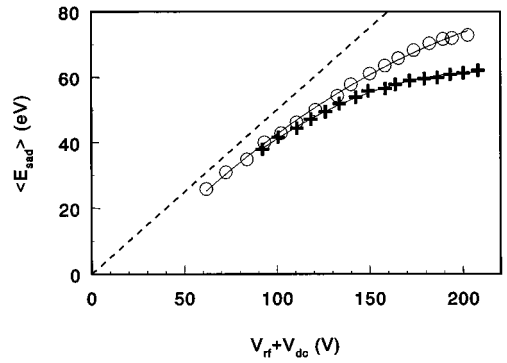

FIG. 16. $\overline{E_{sad}}$ as function of the maximum sheath voltage $V_{rf}+V_{dc}$ in CF_4 plasmas in the normal cavity. The results are determined from the IEDs of CF_3^+. The pressure is 5 mTorr (+) and 20 mTorr (○).

at a certain $\overline{E_{sad}}$: The ion density has to increase with pressure,[8] which is also observed experimentally by Haverlag.[16]

From the measurements the relation between the maximum sheath voltage ($V_{rf}+V_{dc}$) and E_{sad} can be determined. In Fig. 16 this relation is shown for CE_3^+ ions (CF_4 plasma, pressures of 5 and 20 mTorr). In the case where the sheath voltage modulation is purely sinusoidal, so purely capacitive, E_{sad} has to equal $\frac{1}{2}e(V_{rf}+V_{dc})$. The measurements show that $\overline{E}_{sad}$ is less than $\frac{1}{2}e(V_{rf}+V_{dc})$, so we may conclude that the sheath voltage modulation is not sinusoidal at high rf voltages. The deviation from a sinusoidal sheath voltage modulation is larger for low-pressure plasmas in CF_4 where the ion density is higher and the sheath thickness smaller. This conclusion is in agreement with the sheath in argon plasmas where the ion density is the largest for high-pressure plasmas. Consequently, the deviation from a sinusoidal voltage modulation is the largest.[8]

E. Sheath kinetics

To explain the IEDs of the ion species which are present in the sheath of a CF_4 plasma, ion–molecule reactions have to be taken into account. The most important reactions are discussed in this subsection.

Exact data on cross sections of reactions in which CF_2^+ ion species are involved are not available. Therefore, we use the reaction enthalpy as a probe for the reaction rate; as a first estimation in terms of tendencies toward equilibrium, a consideration of the enthalpies can be very useful.

Ions may be produced by ionization of neutrals which collide with electrons or with energetic ions. In the sheath, the contribution of electron impact may be neglected. This is supported by measurements of the IED of the N^+ and N_3^+ ions in a N_2 plasma. Ionization of N and N_3 species by electron impact would generate characteristic features in the IEDs of the N^+ and N_3^+ ions since these newly formed ions start with thermal energy and are accelerated to the electrode surface. From the absence of these features (see Fig. 17) we may conclude that the contribution of electron impact to the newly formed ions in the sheath may be neglected. We extend this conclusion to the CF_4 plasmas, even though the kinetics are more complex than in the N_2 plasma.

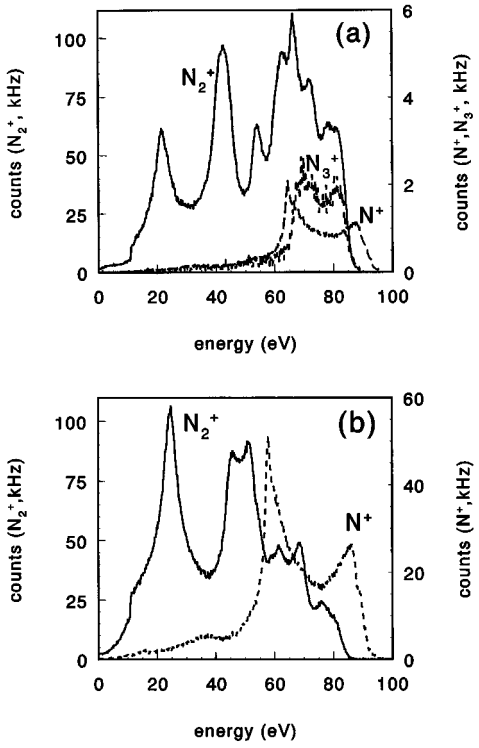

FIG. 17. The IEDs of N_2^+ (solid line), N^+ (dashed line), and N_3^+ ions (dotted line) incident on the grounded electrode in the normal cavity. The rf power injected in the plasma is 69 W and the pressure is (a) 19 mTorr and (b) 76 mTorr.

A neutral atom or molecule can only be ionized by an ion if the energy is a few keV. These energies cannot be obtained in the sheath of a rf plasma. Therefore, ionization of neutrals by highly energetic ions cannot occur in the sheath.

The ions which are present in the plasma can collide with a CF_4 molecule and a fluorine atom transfer reaction may take place (disproportionation reactions). The following reactions can be distinguished. For an endothermic reaction the enthalpy difference[28,29] is added on the left-hand side. For an exothermic reaction the reaction enthalpy[28,29] is added on the right-hand side,

$$CF_3^+ + CF_4 + 6.20\ \text{eV} \rightarrow CF_4^+ + CF_3, \tag{3}$$

$$CF_2^+ + CF_4 \rightarrow CF_3^+ + CF_3 + 0.52\ \text{eV}, \tag{4}$$

$$CF^+ + CF_4 + 0.30\ \text{eV} \rightarrow CF_3^+ CF_2, \tag{5}$$

$$C^+ + CF_4 \rightarrow CF_3^+ + CF + 1.78\ \text{eV}, \tag{6}$$

$$F^+ + CF_4 \rightarrow CF_3^+ + F_2 + 4.29\ \text{eV}. \tag{7}$$

In reaction (3) a CF_4^+ ion is formed. This ion, however, directly decomposes into CF_3^+ and F.[28] The exothermic reactions sometimes occur spontaneously. The endothermic reactions may occur when the energy difference is supplied by the accelerated ion in the sheath.

Also charge exchange reactions may occur in the sheath. The cross sections of charge exchange reactions between two identical species (symmetric charge exchange) are quite large ($\approx 10^{-18}$ m^2). The cross sections of charge exchange reactions between not-identical species (asymmetric charge

exchange) is in general smaller than for symmetric charge exchange ($\approx 10^{-21}$ m^2).[20,30] This mainly is the consequence of the energy difference δE between the ionization levels of the involved ions. In the case of resonant (i.e., $\delta E = 0$) asymmetric charge exchange the cross section can be of the same order of magnitude as for symmetric charge exchange reactions.

We consider the following symmetric (resonant) charge exchange reactions:

$$CF_3^+ + CF_3 \rightarrow CF_3 + CF_3^+, \tag{8}$$

$$CF_2^+ + CF_2 \rightarrow CF_2 + CF_2^+, \tag{9}$$

$$CF^+ + CF \rightarrow CF + CF^+, \tag{10}$$

$$F^+ + F \rightarrow F + F^+. \tag{11}$$

Asymmetric charge exchange reactions will mainly take place between an ion and a CF_4 neutral. We distinguish the following asymmetric charge exchange densities:

$$CF_3^+ + CF_4 + 6.2\ \text{eV} \rightarrow CF_3 + CF_4^+, \tag{12}$$

$$CF_2^+ + CF_4 + E \rightarrow CF_2 + CF_4^+, \tag{13}$$

$$CF^+ + CF_4 + 6.3\ \text{eV} \rightarrow CF + CF_4^+, \tag{14}$$

$$F^+ + CF_4 + 2.7\ \text{eV} \rightarrow F + CF_4^+. \tag{15}$$

The energy difference for reaction (13) is unknown.

The probability that the reactions (3)–(15) occur in the sheath depends on the cross sections and on the densities of the neutrals. The densities of the CF_3, CF_2, and CF neutrals are of the order 10^{18}–10^{19} m^{-3}.[17] The density of the F radicals is of the order of 2.5×10^{19} m^{-3}.[17] The densities of all these species are much lower than the CF_4 neutral density (1.6×10^{20}–5.3×10^{21} m^{-3}); however, due to the larger cross sections for resonant charge exchange, the reaction rates of both types of charge exchange will be comparable.

The next ion–molecule reactions which we discuss are dissociation reactions of CF_n^+ ions by a collision with a neutral, most of the times a CF_4 molecule. We distinguish the following reactions:

$$CF_4 + CF_3^+ + 3.77\ \text{eV} \rightarrow CF_4 + CF_2^+ + F, \tag{16}$$

$$CF_4 + CF_3^+ 8.08\ \text{eV} \rightarrow CF_4 + CF^+ + 2F, \tag{17}$$

$$CF_4 + CF_3^+ + 13.7\ \text{eV} \rightarrow CF_4 + C^+ + 3F, \tag{18}$$

$$CF_4 + CF_2^+ + 5.31\ \text{eV} \rightarrow CF_4 + CF^+ + F, \tag{19}$$

$$CF_4 + CF_2^+ + 10.9\ \text{eV} \rightarrow CF_4 + C^+ + 2F, \tag{20}$$

$$CF_4 + CF^+ + 5.59\ \text{eV} \rightarrow CF_4 + C^+ + F. \tag{21}$$

From the measured IEDs we may conclude which of the reactions (3)–(21) take place in the sheath. The density of F radicals is higher than of CF_2, whereas the CF_2 density is higher than the CF_3 density.[16]

In the previous subsection, from the vanishing of the saddle structure at low pressures we have concluded that there must be an inelastic reaction with a large cross section by which CF_2^+ ions are lost. This may be reaction (4), an exothermic disproportionation reaction. Due to the high density of the CF_4 molecules, the probability that this reaction takes place will be large. The reaction rate can be estimated as follows. At 40 mTorr nearly the whole saddle structure has vanished. The CF_4 density in this case is 2.6×10^{21} m^{-3}. 95% of the CF_2^+ ions will be destroyed when the mean free path is $\frac{1}{3}$ of the sheath thickness. The sheath thickness will be of the order of 2 mm, so the mean free path is 0.7 mm. This gives a cross section of 5×10^{-19} m^2, which is quite reasonable. The charge exchange reactions (9) and (13) also lead to a loss of CF_2^+ ions but their contribution to the total loss will be much smaller than that of reaction (4). At 40 mTorr the mean free path for resonant charge exchange [reaction (9)] is about 12 cm. The mean free path for asymmetric charge exchange [reaction (13)] is about 40 cm. Reactions (3) and (5) are endothermic and their cross section will be small. This can explain why the primary saddle in the IEDs of CF_3^+ and CF^+ ions does not vanish. When the cross section is a factor of 10 smaller, the mean free path is a factor of 10 larger. This means that only 3% of the ions will be destroyed by collision.

From the abundance of low-energy features in the IED of CF_2^+, we have concluded that there must be a reaction by which CF_2^+ ions are produced in the sheath. As shown above, the reaction rates of charge exchange reactions is small. That this reaction is not a dominant production process is confirmed by the fact that no specific charge exchange peaks in the IEDs of the CF_2^+ ions can be observed. Therefore, the dissociation of CF_3^+ ions [reaction (16)] is the most probable production process of CF_2^+ ions in the sheath.

CF_3^+ ions are involved in several reactions. The cross section of resonant charge exchange [reaction (8)] is quite large, but due to the low CF_3 radical density the reaction rate is small (mean free path $\approx$25 cm). Due to the small cross sections, asymmetric charge exchange [reaction (12)] does not have a high rate, either. Therefore, probably CF_3^+ ions are mainly produced in the sheath by the fluorine atom transfer reaction (3) where CF_4^+ decomposes into CF_3^+ and a F radical. The mean free path of this reaction is of the order of 4 mm. The IED of CF_3^+ ions shows some secondary peak structures, although less pronounced than expected for charge exchange. In the IED of CF_3^+ more peak structures can be distinguished than for CF_2^+ due to the longer transit time of the CF_3^+ ions (larger mass).

In the CF^+ case, similar reactions are responsible for the production and loss as for CF_2^+. The difference is that reaction (5) is now slightly endothermic. The consequence is that the ratio between loss and production reactions is different from CF_2^+. Therefore, in the IED of CF^+ the primary saddle structures can be recognized up to higher pressures than for CF_2^+.

F^+ ions are destroyed by the ion transfer reaction.[7] This reaction is exothermic and due to the large CF_4 density the probability for this reaction to occur in the sheath will be quite large. The IEDs of F^+ ions show large peaks, which suggests that resonant charge exchange [reaction (11)] occurs in the sheath. This seems to be quite likely because the F radical density is about five times higher than the CF_3 and CF_2 densities. Furthermore, the cross section for resonant charge exchange is large.

TABLE I. Dominant production and elimination reactions in the sheath of a CF_4 plasma.

Species	Production reaction	Elimination reaction
CF_3^+	disproportionation with CF_4 (3)	dissociation into CF_5^+ (16)
CF_2^+	dissociation of CF_3^+ (16)	disproportionation with CF_4 (4)
CF^+	dissociation of CF_3^+ (17)	disproportionation with CF_4 (5)
F^+	resonant charge exchange with F (11)	disproportionation with CF_4 (7)

V. CONCLUSIONS

The sheath in a CF_4 plasma is far more complex than in an argon or nitrogen plasma. This is due to the number of ion species and to the large variety of ion–molecule reactions.

From the IEDs of the ion species one may conclude which reactions are dominant for the production and loss of the different species in the sheath. These reactions are listed in Table I.

Because most of the elastically scattered ions are not detected, and because there are no reactions by which CHF_2^+ ions can be produced in the sheath, the IEDs of the CHF_2^+ ions mainly represent the ions which have not collided in the sheath. Therefore the IEDs of CHF_2^+ ions may be interpreted as collisionless and can be used to analyze the general sheath behavior.

[1] B. Chapman, *Glow Discharge Processes* (Wiley, New York, 1980).
[2] D. M. Manos and D. L. Flamm, *Plasma Etching, an introduction* (Academic, London, 1989).
[3] J. W. Coburn and E. Kay, J. Appl. Phys. **43**, 4965 (1972).
[4] K. Köhler, J. W. Coburn, D. E. Horne, E. Kay, and J. H. Keller, J. Appl. Phys. **57**, 59 (1985).
[5] A. D. Kuijpers, Ph.D. thesis, University of Utrecht, The Netherlands, 1989.
[6] A. Manenschijn and W. J. Goedheer, J. Appl. Phys. **69**, 2923 (1991).
[7] R. J. M. M. Snijkers, M. J. M. van Sambeek, G. M. W. Kroesen, and F. J. de Hoog, Appl. Phys. Lett. **63**, 308 (1993).
[8] R. J. M. M. Snijkers, Ph.D. thesis, Eindhoven University of Technology Eindhoven, The Netherlands, 1993.
[9] M. J. Kushner, J. Appl. Phys. **58**, 4024 (1985).
[10] D. Vender and R. W. Boswell, IEEE Trans. Plasma Sci. **PS-18**, 725 (1990).
[11] D. Field, D. F. Klemperer, P. W. May, and Y. P. Song, J. Appl. Phys. **70**, 82 (1991).
[12] J. Liu, G. L. Huppert, and H. H. Sawin, J. Appl. Phys. **68**, 3916 (1990).
[13] C. Wild and P. Koidl, J. Appl. Phys. **69**, 2909 (1991).
[14] P. W. May, D. Field, and D. F. Klemperer, J. Appl. Phys. **71**, 3721 (1992).
[15] T. H. J. Bisschops, Ph.D. thesis, Eindhoven University of Technology, The Netherlands, 1987.
[16] M. Haverlag, Ph.D. thesis, Eindhoven University of Technology, The Netherlands, 1991.
[17] D. A. Dahl and J. E. Delmore, *The SIMION PC/PS2 User's Manual Version 4.0* (Idaho National Engineering Laboratory/EG&G Idaho, Inc., Idaho Falls, 1988).
[18] A. Manenschijn, Ph.D. thesis, Delft University of Technology, The Netherlands, 1991.
[19] J. Janes and C. Huth, J. Vac. Sci. Technol. A **10**, 3086 (1992).
[20] E. W. McDaniel, *Collisional Phenomena in Ionized Gases* (Wiley, New York, 1964).
[21] D. Field, D. F. Klemperer, P. W. May, and Y. P. Song, J. Appl. Phys. **70**, 82 (1991).
[22] P. F. Knewstubb and R. Tickner, J. Chem. Phys. **36**, 674 (1962).
[23] J. W. Coburn, Rev. Sci. Instrum. **41**, 1219 (1970).
[24] D. Vender and R. Boswell, IEEE Trans. Plasma Sci. **18**, 725 (1990).
[25] The simulations have been performed with the particle-in-cell simulation program of C. K. Birdsall and A. Langdon [see, e.g., *Plasma Physics Via Computer Simulations* (McGraw–Hill, New York)]. The results are described by J. van Breda in the internal report VDF/NG 92-02, Department of Physics, Eindhoven University of Technology, 1992.
[26] B. E. Thompson, H. H. Sawin, and D. A. Fisher, J. Appl. Phys. **63**, 2241 (1988).
[27] J. Janes, J. Appl. Phys. **74**, 659 (1993).
[28] M. J. K. Pabst, H. S. Tan, and J. L. Franklin, Int. J. Mass Spec. Ion Phys. **20**, 191 (1976).
[29] Ce Ma, M. R. Bruce, and R. A. Bonham, Phys. Rev. A **44**, 2921 (1991).
[30] J. B. Hasted, *Physics of Atomic Collisions* (Butterworths, London, 1964).
[31] T. Nakano and H. Sugai, Jpn. J. Appl. Phys. **31**, 2919 (1992).